

Chaotic pH Oscillations in the Hydrogen Peroxide–Thiosulfate–Sulfite Flow System

Gyula Rábai*

Institute of Physical Chemistry, Kossuth Lajos University, H-4010 Debrecen, Hungary

Ichiro Hanazaki*

Department of Chemistry, Faculty of Science, Hiroshima University, Kagamiyama, Higashi-Hiroshima 739-8526, Japan

Received: May 18, 1999; In Final Form: July 8, 1999

Detailed numerical studies and experiments have revealed that two types of limit cycle pH oscillations with very different frequencies, complex periodic behavior, and chaos are exhibited by a catalyst-free H_2O_2 – $\text{S}_2\text{O}_3^{2-}$ – SO_3^{2-} – H^+ aqueous reaction system in a continuous-flow stirred tank reactor at 20.0 °C. Chaos appears around pH 6 in the case of a small excess of H_2O_2 over the reducing agents in a narrow range of input concentrations and flow rates. The main features of the observed dynamical behavior have been reproduced by a simple chemical mechanism derived from an earlier proposed model of the Cu^{2+} -catalyzed H_2O_2 – $\text{S}_2\text{O}_3^{2-}$ oscillatory reaction. Slow and reversible proton-assisted dehydration of HOS_2O_3^- intermediate to S_2O_3 reactive species and its subsequent reaction with $\text{S}_2\text{O}_3^{2-}$ to form $\text{S}_4\text{O}_6^{2-}$ have been considered in addition to earlier proposed composite reactions.

Introduction

The reaction between H_2O_2 and $\text{S}_2\text{O}_3^{2-}$ in the presence of a catalytic amount of Cu^{2+} ions has long been known to exhibit large-amplitude temporal pH oscillations if it is carried out in a continuous-flow stirred tank reactor (CSTR).¹ Periodic changes in the pH and in the redox potential have been observed in the experiments not only in a CSTR mode but also in a semibatch configuration, where a solution of $\text{Na}_2\text{S}_2\text{O}_3$ along with dilute NaOH is introduced at a constant rate into a mixture containing excess H_2O_2 and a small amount of CuSO_4 .^{2,3} This system is considered to be the first oscillatory reaction in which the key governing kinetic role of the changing hydrogen ion concentration (pH regulation) has been recognized.¹ The Cu^{2+} catalyst has been believed to be a necessary key component of the feedback mechanism needed for oscillations to occur under isothermal conditions in this reaction. However, under quasi-adiabatic conditions, thermokinetic oscillations with large-amplitude temperature variations were found in the absence of any catalyst.⁴ Here, the reaction heat causes a change in the temperature which generates the necessary kinetic feedbacks as the rate of key composite reactions increases with increasing temperature.

In a recent drive to design new chaotic pH oscillators and to understand their mechanism, our attention has been attracted to the H_2O_2 – $\text{S}_2\text{O}_3^{2-}$ reaction. It can exhibit not only simple but also complex periodic changes in the pH; under certain conditions mixed-mode periods are observed in the experiments. Such periods consist of large-amplitude oscillations which are intercalated by a number of small peaks. Pure small-peak oscillations as well as large-amplitude ones have also been found neatly in experiments under different conditions. Such a behavior is often accompanied by chemical chaos. However, chaos has not yet been reported in this reaction.

Recently, Kurin-Csorgei et al. have proposed a chemical model for the Cu^{2+} -catalyzed isothermal system which accounts for both the batch behavior and the oscillations and bistability observed in a CSTR.⁵ Multiphase mixed-mode periods could

also be calculated by the extended version of the proposed scheme. Here, chemically well-grounded composite reactions are considered. The capability of the thiosulfate ion to be partially oxidized to relatively stable intermediates (such as HOS_2O_3^- , $\text{S}_4\text{O}_6^{2-}$, SO_3^{2-}) prior to its total oxidation to sulfate ion by H_2O_2 is the main feature of the scheme. However, the necessity of varying the hypothetical values of some rate constants to reproduce different kinds of behavior implies that the model is still not complete. Nevertheless, we think that the basic concept of the model is probably correct and deserves further analysis. It contains very interesting feedback channels that might be the source of more complex dynamical behavior, such as burst oscillations and chaos, if the parametric conditions⁶ (values of the rate constants) were favorable for such dynamics.

The main question we address in the present work is whether this scheme can, indeed, fulfill the mechanistic conditions⁶ of chaotic behavior in a flow system. If yes, it is also to be answered whether such behavior can be found in the experiments. To answer these questions, first we examine the proposed mechanism in more detail. We disclose that, contrary to the experiments, the proposed scheme produces oscillations and chaos even when the Cu^{2+} -containing term is eliminated from the rate laws. Then, we separate two submechanisms to show that the scheme contains at least two simple oscillators. The complexity of the calculated dynamical behavior is explained by coupling of the two limit cycle core oscillators, which are involved in the original mechanism. We discuss the possible reason for why oscillations do not occur in the experiments when no Cu^{2+} is present. Then, we report on the experimental discovery of mix-mode and chaotic oscillations in the catalyst-free reaction system when some SO_3^{2-} is introduced into the reactor along with H_2O_2 , $\text{S}_2\text{O}_3^{2-}$, and H^+ . Finally, we propose a modified version of the mechanism to describe better the observed behavior.

Experimental Section

Materials. Reagent grade H_2O_2 , H_2SO_4 , Na_2SO_3 , and $\text{Na}_2\text{S}_2\text{O}_3$ (all KATAYAMA) were used without further purification.

Doubly distilled water used in preparing solutions was first purged with N_2 for elimination of O_2 and CO_2 impurities. CO_2 impurities should be avoided with care because it can be the source of a negative feedback in a pH oscillator.⁷ Two input solutions were prepared daily: one contained H_2O_2 and the other contained the necessary amount of Na_2SO_3 , $\text{Na}_2\text{S}_2\text{O}_3$, and H_2SO_4 . With this combination, we could avoid random local acidification in the CSTR during mixing. Since the hydrogen ion is the autocatalyst, local acidification by the input solutions should be avoided carefully in the reactor, because such an acidification can initiate the autocatalytic reaction randomly. Since it was essential to avoid autoxidation of S(IV) in the reservoir, its solution was kept from air, but not bubbled to avoid the loss of the volatile components. Had this solution in the reservoir been bubbled, some loss of SO_2 would have been unavoidable despite of the slightly alkaline pH. Both input solutions had been stored at $20.0\text{ }^\circ\text{C}$ for 12 h before use, and they were discarded after 24 h storage. This care was necessary in order to obtain reproducible results. For example, the period of the oscillations was longer when freshly prepared sulfite solution was used than in the case of an old sulfite solution. The concentration of H_2O_2 was determined with permanganate solution; the sulfite and thiosulfate solutions were titrated with a standardized iodine solution. The sulfite source may contain some NaHSO_3 or some alkaline impurities which modify strongly the dynamical behavior.

Reactor. The continuous flow experiments were performed in a water-jacketed cylindrical-shaped glass vessel with a liquid volume of 13.9 mL. The reactor was sealed with a silicon cap in all the experiments. A pH electrode, the input (i.d. 1.0 mm) and output tubes (i.d. 2.0 mm) were led through the cap. A Teflon-covered magnetic stirrer (1 cm long) was used to ensure uniform mixing at around 500 rpm.

Procedure. Most of the experiments were carried out at $20.0 \pm 0.1\text{ }^\circ\text{C}$. The temperature should be controlled very carefully, because the dynamical behavior of the system is very sensitive to it. The reactor was fed with prethermostated input solutions by means of a peristaltic pump (EYELA). The excess liquid was removed with the same pump. The liquid level could be controlled by the vertical position of the outlet tubes. The pH and the temperature inside the reactor were continuously measured. The experiments were started by filling the reactor with the input solutions at the highest pump speed available (5.0 mL/min). After the reactor had been filled, the pump speed was reduced to the desired value. pH–time data were collected by a computer and were recorded on a disk.

Computation. A semiimplicit Runge–Kutta method⁸ with an error parameter of 10^{-5} was used for numerical integrations. This low value of the error parameter was proved to be necessary and sufficient for obtaining correct results.

Results and Discussion

About the Model. Summarized in Table 1 is a simplified version of an oscillatory model developed by Kurin–Csorgei et al.⁵ for the copper-catalyzed isothermal reaction. The rate laws along with the corresponding set of rate constant values are also shown in Table 1. Most of the composite reactions are obviously not elementary steps, so the corresponding rate laws may contain more than one term. The second term of $\text{M1}'$ in the cited reference⁵ describes the direct catalytic effect of Cu^{2+} on the H_2O_2 oxidation of $\text{S}_2\text{O}_3^{2-}$. Since we limit our present considerations to a catalyst-free system, we neglect the Cu^{2+} -containing term and take into account a one-term rate equation for M1 as shown in Table 1. Note that the dissociation

TABLE 1: Composite Reactions, Their Empirical Rate Laws, and Rate Constant Values of the $\text{H}_2\text{O}_2\text{--S}_2\text{O}_3^{2-}\text{--SO}_3^{2-}\text{--H}^+$ Reaction System

reactions	
$\text{H}_2\text{O}_2 + \text{S}_2\text{O}_3^{2-} \rightarrow \text{HOS}_2\text{O}_3^- + \text{OH}^-$	(M1)
$\text{H}_2\text{O}_2 + \text{HOS}_2\text{O}_3^- \rightarrow 2\text{HSO}_3^- + \text{H}^+$	(M2)
$\text{S}_2\text{O}_3^{2-} + \text{HOS}_2\text{O}_3^- \rightarrow \text{S}_4\text{O}_6^{2-} + \text{OH}^-$	(M3)
$\text{H}_2\text{O} \rightleftharpoons \text{H}^+ + \text{OH}^-$	(M4)
$\text{S}_4\text{O}_6^{2-} + \text{H}_2\text{O}_2 \rightarrow 2\text{HOS}_2\text{O}_3^{2-}$	(M5)
$\text{H}_2\text{O}_2 + \text{HSO}_3^- \rightarrow \text{SO}_4^{2-} + \text{H}_2\text{O} + \text{H}^+$	(M6)
$\text{H}_2\text{O}_2 + \text{SO}_3^{2-} \rightarrow \text{SO}_4^{2-} + \text{H}_2\text{O}$	(M7)
$\text{HSO}_3^- \rightleftharpoons \text{H}^+ + \text{SO}_3^{2-}$	(M8)

rate constants	
rate laws	(k_i in $\text{M}^{-1}\text{ s}^{-1}$; k'_i in $\text{M}^{-2}\text{ s}^{-1}$)
$v_1 = k_1[\text{H}_2\text{O}_2][\text{S}_2\text{O}_3^{2-}]$	$k_1 = 0.019$
$v_2 = k_2[\text{H}_2\text{O}_2][\text{HOS}_2\text{O}_3^-]$	$k_2 = 0.020$
$v_3 = (k_3 + k'_3[\text{H}^+])[\text{S}_2\text{O}_3^{2-}][\text{HOS}_2\text{O}_3^-]$	$k_3 = 1.0, k'_3 = 1.0 \times 10^5$
$v_4 = k_4[\text{H}_2\text{O}]$	$k_4[\text{H}_2\text{O}] = 1.0 \times 10^{-3}\text{ M s}^{-1}$
$v_{-4} = k_{-4}[\text{H}^+][\text{OH}^-]$	$k_{-4} = 1.0 \times 10^{11}$
$v_5 = (k_5 + k'_5[\text{OH}^-])[\text{H}_2\text{O}_2][\text{S}_4\text{O}_6^{2-}]$	$k_5 = 0.07, k'_5 = 5.0 \times 10^4$
$v_6 = (k_6 + k'_6[\text{H}^+])[\text{H}_2\text{O}_2][\text{HSO}_3^-]$	$k_6 = 7.0, k'_6 = 1.48 \times 10^7$
$v_7 = k_7[\text{H}_2\text{O}_2][\text{SO}_3^{2-}]$	$k_7 = 0.20$
$v_8 = k_8[\text{HSO}_3^-]$	$k_8 = 3.0 \times 10^3\text{ s}^{-1}$
$v_{-8} = k_{-8}[\text{H}^+][\text{SO}_3^{2-}]$	$k_{-8} = 5.0 \times 10^{10}$

equilibrium of H_2O_2 to H^+ and HO_2^- was taken into account in the original model.⁵ Here we neglect this equilibrium, because it has a very limited influence on the calculated behavior when the excess of H_2O_2 is not high and the pH is below 10. These conditions apply to the present work.

Other features of the original mechanism as well as the rate constant values have been preserved for the first calculations of expected dynamical behavior in a catalyst-free reaction. Note that not only the overall rate, but also the ratio of the rate of the composite reactions might be affected by the catalyst. As we will show later, such an effect may cause significant disagreement between the calculated and experimental kinetic behavior in the absence of catalyst.

Calculated Chaos in a Catalyst-Free $\text{H}_2\text{O}_2\text{--S}_2\text{O}_3^{2-}$ Reaction in a CSTR. Preliminary calculations have revealed some new features of the model shown in Table 1. First, it turned out that the Cu^{2+} -containing rate term of v_1 in the original version⁵ is not essential for oscillations. Second, the model is capable of producing two types of regular oscillations with very different frequencies at different flow rates, even when the input concentrations are chosen to be the same. The combination of the two frequencies results in complex periodic and chaotic solutions under appropriate initial conditions. Typical calculated pH–time series ($[\text{H}_2\text{O}_2]_0 = 0.030$, $[\text{S}_2\text{O}_3^{2-}]_0 = 0.005$, $[\text{H}^+]_0 = 0.001\text{ M}$) are shown in Figure 1 as examples. On one hand, low-frequency, high-amplitude oscillations were calculated at relatively high flow rate values ($k_0 = 15.0 \times 10^{-4}\text{ s}^{-1}$, Figure 1, top). On the other hand, high-frequency, small-amplitude oscillations could be calculated with slow flow rate ($k_0 = 7.0 \times 10^{-4}\text{ s}^{-1}$, Figure 1, bottom). At middle flow rate, complex periodic (two-peak periods at $k_0 = 10 \times 10^{-4}\text{ s}^{-1}$) and chaotic pH–time series were obtained ($k_0 = 8.5 \times 10^{-4}\text{ s}^{-1}$, Figure 1, middle).

Now we address the interesting question of which parts of the model are responsible for the two different types of calculated oscillations. At least two autocatalytic cycles can easily be recognized in the model shown in Table 1. Both are expected to produce limit cycle oscillations under flow conditions if an appropriate negative feedback is connected to them with a time delay. Therefore, it seems to be possible to extract two core oscillatory mechanisms separately responsible for the two frequencies that compose the complex oscillations.

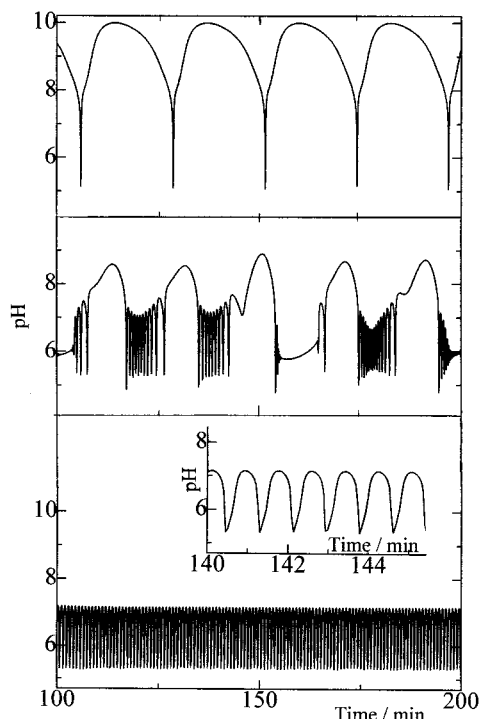


Figure 1. Calculated fractions of different types of pH oscillations in a CSTR mode at different flow rates. Calculations were carried out on the basis of the mechanism and rate constants shown in Table 1. Concentrations in the combined input feed were $[\text{H}_2\text{O}_2]_0 = 0.030$, $[\text{S}_2\text{O}_3^{2-}]_0 = 0.0050$, $[\text{H}^+]_0 = 0.0010$ M. Normalized flow rate was $k_0 = 15.0 \times 10^{-4}$ (top, low-frequency oscillations), 8.5×10^{-4} (middle, chaos), and $7.0 \times 10^{-4} \text{ s}^{-1}$ (bottom, high-frequency oscillations). The insert in the bottom shows the high-frequency oscillations on an extended time scale.

TABLE 2: Core I Oscillator

reactions	
$\text{H}_2\text{O}_2 + \text{HSO}_3^- \rightarrow \text{SO}_4^{2-} + \text{H}_2\text{O} + \text{H}^+$	(M6)
$\text{S}_2\text{O}_3^{2-} + \text{HOS}_2\text{O}_3^- \rightarrow \text{S}_4\text{O}_6^{2-} + \text{OH}^-$	(M3)
$\text{H}_2\text{O} \rightleftharpoons \text{H}^+ + \text{OH}^-$	(M4)
$\text{HSO}_3^- \rightleftharpoons \text{H}^+ + \text{SO}_3^{2-}$	(M8)
rate laws ^a	
$v_6 = k_6'[\text{H}^+][\text{H}_2\text{O}_2][\text{HSO}_3^-]$	
$v_3 = k_3'[\text{H}^+][\text{S}_2\text{O}_3^{2-}][\text{HOS}_2\text{O}_3^-]$	

^a v_4, v_{-4}, v_8, v_{-8} , and the values of rate constants are the same as in Table 1.

Core I Oscillator. One of the positive feedbacks is the autocatalytic oxidation of HSO_3^- which operates under slightly acidic conditions. The species responsible for the autocatalysis is H^+ . HSO_3^- is produced in reaction M2 as an intermediate. Its oxidation to SO_4^{2-} by H_2O_2 in reaction M6 produces H^+ , and the corresponding reaction rate v_6 increases with increasing concentration of H^+ . If we consider reactions M3 (as negative feedback for H^+) along with reaction M6 (as positive feedback mediated by H^+) and we take into account dissociation equilibria M4 and M8, which introduce time delay between the negative and the positive feedbacks, we can separate a core oscillatory mechanism (core I oscillator) from the scheme in Table 1. Core I oscillator is shown in Table 2. For simplicity, here we consider only the second terms of the rate equations for both reactions M3 and M6, because the first terms do not play any significant role in the feedback mechanism responsible for oscillations. Of course, to make this simple hypothetical scheme workable, an input feed should contain SO_3^{2-} and HOS_2O_3^- in addition to $\text{S}_2\text{O}_3^{2-}$, H^+ , and H_2O_2 because no chemical sources of SO_3^{2-}

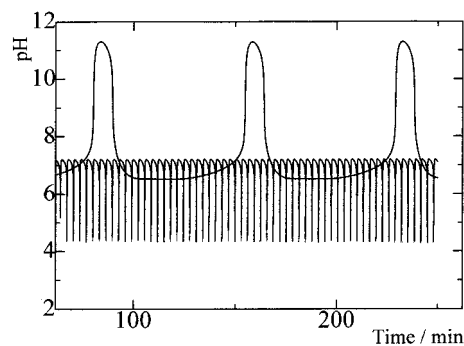


Figure 2. pH–time series calculated by the core oscillatory mechanisms. High frequencies were obtained by the core I mechanism shown in Table 2 with $[\text{H}_2\text{O}_2]_0 = 0.010$ M. Low frequencies were calculated by the core II scheme shown in Table 3 with $[\text{H}_2\text{O}_2]_0 = 0.040$ M. Other input concentrations were $[\text{S}_2\text{O}_3^{2-}]_0 = 0.010$, $[\text{H}^+]_0 = 0.0010$, $[\text{HOS}_2\text{O}_3^-]_0 = 0.0020$, $[\text{SO}_3^{2-}]_0 = 0.0020$ M; $k_0 = 5.0 \times 10^{-4} \text{ s}^{-1}$ in both cases.

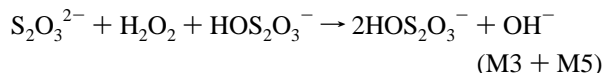
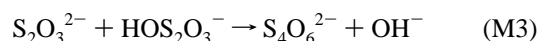
TABLE 3: Core II Oscillator

reactions	
$\text{S}_2\text{O}_3^{2-} + \text{HOS}_2\text{O}_3^- \rightarrow \text{S}_4\text{O}_6^{2-} + \text{OH}^-$	(M3)
$\text{S}_4\text{O}_6^{2-} + \text{H}_2\text{O}_2 \rightarrow 2\text{HOS}_2\text{O}_3^-$	(M5)
$\text{H}_2\text{O}_2 + \text{HOS}_2\text{O}_3^- \rightarrow 2\text{HSO}_3^- + \text{H}^+$	(M2)
$\text{H}_2\text{O}_2 + \text{SO}_3^{2-} \rightarrow \text{SO}_4^{2-} + \text{H}_2\text{O}$	(M7)
$\text{H}_2\text{O} \rightleftharpoons \text{H}^+ + \text{OH}^-$	(M4)
$\text{HSO}_3^- \rightleftharpoons \text{H}^+ + \text{SO}_3^{2-}$	(M8)
rate laws ^a	
$v_3 = k_3[\text{S}_2\text{O}_3^{2-}][\text{HOS}_2\text{O}_3^-]$	
$v_5 = k_5'[\text{OH}^-][\text{H}_2\text{O}_2][\text{S}_4\text{O}_6^{2-}]$	

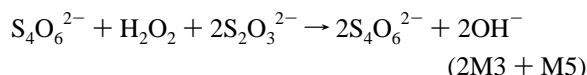
^a $v_2, v_4, v_{-4}, v_7, v_8, v_{-8}$, and the values of rate constants are shown in Table 1.

and HOS_2O_3^- are involved in the core. Calculations show that the core I oscillator scheme can generate high-frequency oscillations around pH 6 (Figure 2).

Core II Oscillator. Reactions M3 and M5 constitute another important autocatalytic cycle in the model. Their sum shows a multiplication of HOS_2O_3^- in each cycle:



Similarly another autocatalytic buildup of $\text{S}_4\text{O}_6^{2-}$ may also be shown by the sum of $2\text{M3} + \text{M5}$.



There are other interesting feedbacks in reactions M3 and M5 as OH^- produced in M3 decreases the rate of M3 through the water dissociation equilibrium, because v_3 is a dependent on $[\text{H}^+]$ (autoinhibition). However, this feedback seems to have minor contribution to the periodic behavior. At the same time, increasing concentration of OH^- increases the rate of M5 (cross catalysis). Obviously, reactions M2 and M7 serve as negative feedbacks, because M2 removes HOS_2O_3^- from the autocatalytic cycle and M7 reduces the buffering capacity of M8 equilibrium by removing some SO_3^{2-} . Summarized in Table 3 are the reactions and rate laws considered for core II oscillator. Again, for simplicity we have neglected the rate terms that are

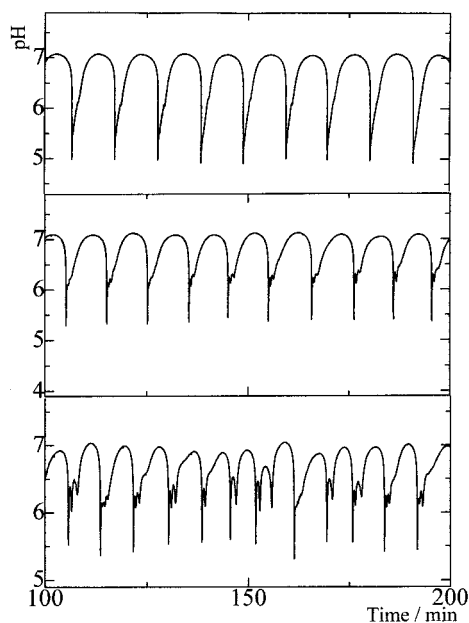


Figure 3. Measured oscillations at different flow rates in the catalyst-free $\text{H}_2\text{O}_2\text{-S}_2\text{O}_3^{2-}\text{-SO}_3^{2-}\text{-H}^+$ system. Observe the development of chaos (bottom) from low frequencies (top) with increasing flow rate. Input concentrations: $[\text{H}_2\text{O}_2]_0 = 0.0097$, $[\text{S}_2\text{O}_3^{2-}]_0 = 0.0048$, $[\text{H}^+]_0 = 0.0010$, $[\text{SO}_3^{2-}]_0 = 0.0025$ M; $k_0 = 4.69 \times 10^{-4}$ (top), 5.03×10^{-4} (middle), and $5.24 \times 10^{-4} \text{ s}^{-1}$ (bottom).

not essential for oscillations to occur. Long periods in the high-pH region could be calculated by core II mechanism. An example is shown in Figure 2 along with the high-frequency oscillations calculated by the core I mechanism.

We suggest that the cross-effect between the two oscillatory submechanisms should be the source of the calculated complex periodic and chaotic behavior obtained on the basis of the whole scheme (Figure 1). For example, reaction M2 supplies HSO_3^- for core I while it removes HOS_2O_3^- from the core II oscillator. There are also strong interactions between other composite reactions of the model through H^+ and OH^- ions because they are common components of most of the composite reactions.

Results of Experiments

Despite predictions by the model discussed in the preceding paragraphs, neither simple nor complex oscillations have yet been found experimentally under isothermal conditions in the absence of catalyst. We performed systematic experiments to search for oscillations in a wide parameter space. In agreement with a previous report,¹ we found no oscillations in the catalyst-free $\text{H}_2\text{O}_2\text{-S}_2\text{O}_3^{2-}$ reaction in a CSTR at 20.0 °C in the input concentration range $[\text{H}_2\text{O}_2]_0 = 0.005\text{-}0.050$ M, $[\text{S}_2\text{O}_3^{2-}]_0 = 0.002\text{-}0.050$ M, $[\text{H}^+]_0 = 5.0 \times 10^{-4} \text{-} 0.01$ M, and at $k_0 = 5.0 \times 10^{-4} \text{-} 4.0 \times 10^{-3} \text{ s}^{-1}$ flow rate range. Some experiments have been performed at 30.0 and 40.0 °C without success of finding oscillations. However, the system can be forced to an oscillatory state by adding some SO_3^{2-} to the input feed. SO_3^{2-} is an important intermediate of the oxidation of $\text{S}_2\text{O}_3^{2-}$, and its introduction increases the contribution of core I oscillator to the overall dynamics.

With this modification, both simple and complex oscillations in pH could easily be observed in the CSTR experiments at 20.0 °C. Shown in Figure 3 are typical time series measured at different flow rates at an optimized input concentration ratio. To obtain oscillatory responses, a small excess of H_2O_2 over the reducing agents was necessary in the input feed, but high excess is not favorable. $\text{S}_2\text{O}_3^{2-}$ should be in excess over both

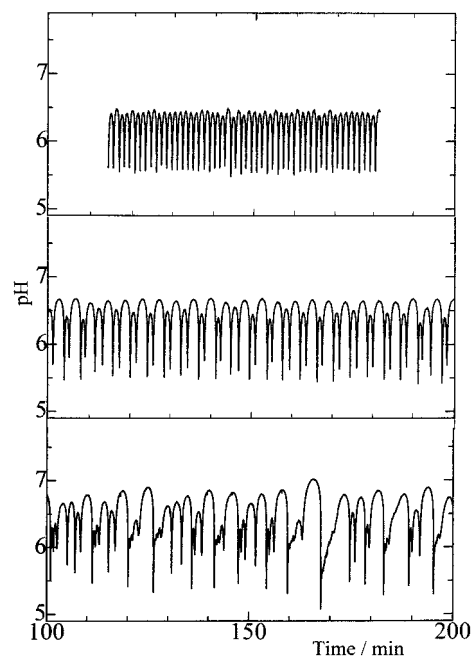


Figure 4. Experimental period doubling from high frequencies to chaos. $k_0 = 7.39 \times 10^{-4}$ (top, high frequencies), 5.89×10^{-4} (middle, mostly period 2 with some irregularity), $5.51 \times 10^{-4} \text{ s}^{-1}$ (bottom, chaos). Input concentrations are the same as in Figure 3.

H^+ and SO_3^{2-} , while the input concentration of SO_3^{2-} should exceed that of $[\text{H}^+]$. Low-frequency oscillations were obtained at low flow rate (Figure 3, top). With increasing flow rate, small peaks appear between the large ones producing somewhat irregular, mostly P3 oscillations (Figure 3, middle, each period consists of three peaks). A fraction of chaotic time series is shown in the bottom of Figure 3 that was obtained with increasing further the flow rate. Chaos with more small peaks were measured at $k_0 = 5.51 \times 10^{-4} \text{ s}^{-1}$ (Figure 4, bottom). When the flow rate is set even higher, period 2 oscillations were obtained (Figure 4, middle). Period 2 is accompanied by some irregularities because the behavior is very sensitive to the experimental conditions and we were not able to control the conditions better. High-frequency oscillations are shown on the top of Figure 4. Finally, a steady state sets in around pH 5 at high flow rate.

An analysis of the measured chaotic time series was carried out to decide whether the observed irregular oscillation is of deterministic origin or due to some unnoticed random perturbation of the reactor. A cap-shaped next return map has been obtained when the pH of a maximum was delineated as a function of the pH of the previous maximum (Figure 5). The next return map and the results of other data analysis also support that the chaos is of deterministic origin in the present system.

Both regular and chaotic oscillations appear in a rather small region of the parameter space. A typical state diagram spanned in the $k_0\text{-}[\text{S}_2\text{O}_3^{2-}]_0$ plane is presented in Figure 6. Complex periodic oscillations and chaos are found in the shaded part inside the oscillatory region. Reproducibility of the behavior is acceptable. However, when Na_2SO_3 or H_2O_2 were taken from new jars, some shift of the oscillatory and chaotic region in the parameter space was observed in the experiments. We reproduced some chaotic traces using another CSTR (23.4 mL liquid volume) with a longer stirrer bar and a new peristaltic pump. The temperature should be controlled very carefully because the dynamical behavior of the system is extremely sensitive to even a small change (0.5 °C) in the temperature.

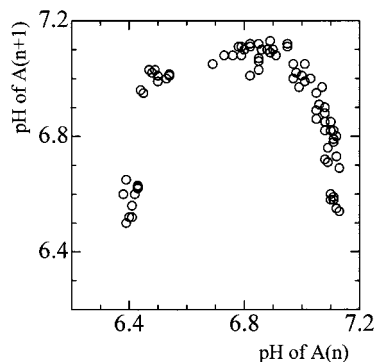


Figure 5. Measured pH maximum as a function of the pH in the previous maximum (next return map). Data have been collected in a CSTR run for 400 min. Input concentrations: $[\text{H}_2\text{O}_2]_0 = 0.0097$, $[\text{S}_2\text{O}_3^{2-}]_0 = 0.0048$, $[\text{H}^+]_0 = 0.0010$, $[\text{SO}_3^{2-}]_0 = 0.0025$ M; $k_0 = 5.68 \times 10^{-4} \text{ s}^{-1}$.

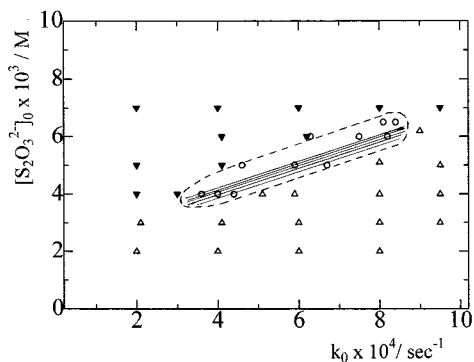


Figure 6. Experimental state diagram. Narrow range of oscillatory states is indicated by open circles, triangles indicate steady states around pH 5 (Δ) and pH between 7.5 and 8.5 (\blacktriangledown). Complex periodic and chaotic behavior can be measured in the shaded area inside the oscillatory regime. Fixed parameters: $[\text{H}_2\text{O}_2]_0 = 0.0097$, $[\text{H}^+]_0 = 0.0010$, $[\text{SO}_3^{2-}]_0 = 0.0025$ M.

Modified Mechanism for the Catalyst-Free Chaotic H_2O_2 – $\text{S}_2\text{O}_3^{2-}$ – SO_3^{2-} – H^+ Flow System. To reproduce the observed behavior in a catalyst-free system, the model suggested by Kurin-Csorgei et al.⁵ for the Cu^{2+} -catalyzed reaction between H_2O_2 and $\text{S}_2\text{O}_3^{2-}$ should be modified. Catalysis by Cu^{2+} is taken into account in the original model with a rate term in ν_1 . However, the effect of Cu^{2+} is not likely to be confined only to this composite reaction. There are more composite reactions that seem to be much slower in the absence of Cu^{2+} catalyst than in its presence. Probably this is the main reason the model cannot reproduce properly the behavior of the catalyst-free system, even if the $[\text{Cu}^{2+}]$ -containing rate term is removed from the scheme. Our experiments have revealed that the noncatalyzed oxidation of $\text{S}_4\text{O}_6^{2-}$ (M5) is much slower than indicated in Table 1. It is too slow to have significant contribution to the overall dynamics under the experimental conditions applied in the present study (pH below 7, only small excess of H_2O_2). Reaction M7 is also much slower than reaction M6 in the pH range of oscillations because sulfur(IV) exists mostly in the form HSO_3^- rather than in SO_3^{2-} . In addition, k_7 is much smaller than k_6 . For these reasons, we neglect both M5 and M7 in our further considerations. We assign a smaller rate constant for M2, which may also be justified by the lack of the catalyst. The rate constants k_6 and k_6' should also be smaller at 20.0 °C than their values measured at 25.0 °C. The most important modification is the introduction of reaction M9, which is a H^+ -assisted dehydration of HOS_2O_3^- to form S_2O_3 . S_2O_3 species is often described in the literature and even in simple textbooks

TABLE 4: Modified Mechanism of the Chaotic Oscillation in the Catalyst-Free H_2O_2 – $\text{S}_2\text{O}_3^{2-}$ – SO_3^{2-} – H^+ Flow System

reactions	
$\text{H}_2\text{O}_2 + \text{S}_2\text{O}_3^{2-} \rightarrow \text{HOS}_2\text{O}_3^- + \text{OH}^-$	(M1)
$\text{H}_2\text{O}_2 + \text{HOS}_2\text{O}_3^- \rightarrow 2\text{HSO}_3^- + \text{H}^+$	(M2)
$\text{S}_2\text{O}_3^{2-} + \text{S}_2\text{O}_3 \rightarrow \text{S}_4\text{O}_6^{2-}$	(M3b)
$\text{H}_2\text{O} \rightleftharpoons \text{H}^+ + \text{OH}^-$	(M4)
$\text{H}_2\text{O}_2 + \text{HSO}_3^- \rightarrow \text{SO}_4^{2-} + \text{H}_2\text{O} + \text{H}^+$	(M6)
$\text{HSO}_3^- \rightleftharpoons \text{H}^+ + \text{SO}_3^{2-}$	(M8)
$\text{HOS}_2\text{O}_3^- + \text{H}^+ \rightleftharpoons \text{S}_2\text{O}_3 + \text{H}_2\text{O}$	(M9)

rate laws	rate constants (k_i in $\text{M}^{-1} \text{ s}^{-1}$)
$\nu_1 = k_1[\text{H}_2\text{O}_2][\text{S}_2\text{O}_3^{2-}]$	$k_1 = 0.019$
$\nu_2 = k_2[\text{H}_2\text{O}_2][\text{HOS}_2\text{O}_3^-]$	$k_2 = 0.010$
$\nu_3 = k_{3b}[\text{S}_2\text{O}_3^{2-}][\text{S}_2\text{O}_3]$	$k_{3b} = 5.0$
$\nu_4 = k_4[\text{H}_2\text{O}]$	$k_4[\text{H}_2\text{O}] = 1.0 \times 10^{-3} \text{ M s}^{-1}$
$\nu_{-4} = k_{-4}[\text{H}^+][\text{OH}^-]$	$k_{-4} = 1.0 \times 10^{11}$
$\nu_6 = (k_6 + k_6'[\text{H}^+])[\text{H}_2\text{O}_2][\text{HSO}_3^-]$	$k_6 = 4.0, k_6' = 1.0 \times 10^7$
$\nu_8 = k_8[\text{HSO}_3^-]$	$k_8 = 3.0 \times 10^3 \text{ s}^{-1}$
$\nu_{-8} = k_{-8}[\text{H}^+][\text{SO}_3^{2-}]$	$k_{-8} = 5.0 \times 10^{10}$
$\nu_9 = k_9[\text{HOS}_2\text{O}_3^-][\text{H}^+]$	$k_9 = 1.0 \times 10^3$
$\nu_{-9} = k_{-9}[\text{S}_2\text{O}_3]$	$k_{-9} = 0.020 \text{ s}^{-1}$

as solid crystals, but it decomposes in dilute aqueous solutions rather quickly. Its transient formation as a reactive intermediate has been assumed in the mechanism of the oxidation of thiosulfate.^{9,10} In reaction M3, two negative ions react with each other as proposed by Schiller.¹¹ Here we replaced composite reaction M3 by M3b in which neutral S_2O_3 reacts with a negative $\text{S}_2\text{O}_3^{2-}$ to produce tetrathionate. M3b seems to be a more favorable reaction than M3. The modified mechanism is presented in Table 4. The dynamic structure of the modified version differs significantly from that of the original version shown in Table 1, but a critical governing role of $[\text{H}^+]$ is obviously common in both versions. Only one H^+ -producing autocatalytic reaction (M6) is considered in the modified scheme, but two H^+ -consuming negative feedbacks operate (M1 and M9 + M3b). Reactions M1 and M3b are separated in time by the slow reaction M9. Equilibrium M8 introduces time delay between the positive and negative feedback channels. Such a multichannel negative feedback has been shown to be the source of chemical chaos.¹²

In agreement with experiments, we found that this mechanism did not produce oscillations in a catalyst-free H_2O_2 – $\text{S}_2\text{O}_3^{2-}$ reaction in the studied parameter space unless SO_3^{2-} is introduced into the input feed. Furthermore, it is capable of describing simple oscillations with very different frequencies, period doubling bifurcations, and chaos similar to that found experimentally in the H_2O_2 – $\text{S}_2\text{O}_3^{2-}$ – SO_3^{2-} reaction at the same input concentrations and at similar flow rates. (Figures 7 and 8). Of course, the mechanism is too simple to describe all the details of the dynamical behavior. The calculated amplitudes are somewhat higher than their measured counterparts. The calculated range of oscillations is also significantly wider than the measured one. A calculated next return map is presented in Figure 9, which is similar to that found experimentally (Figure 5), but a group of experimental points in the region of small pH maxima is not found in the simulated map. A comparison of the maps also indicates that the measured pH maxima are located in a more narrow range of pH than the calculated ones. Despite this, we think that the modified mechanism gives a reasonable description of the very complex dynamical behavior of the system. It may be surprising how simple this mechanism is. Nevertheless, we intend to study further this reaction system and improve its mechanism.

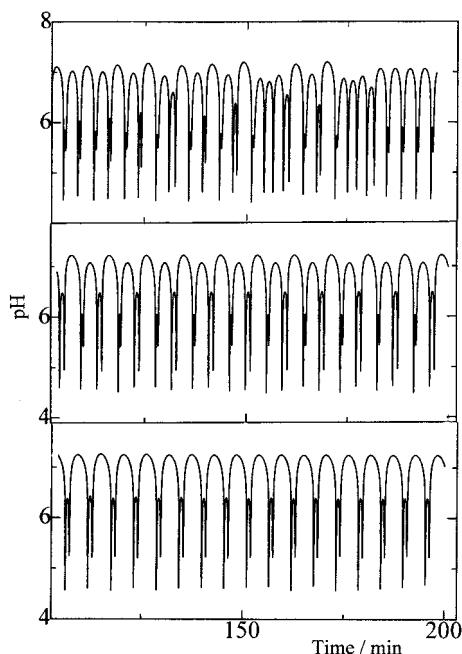


Figure 7. Calculated fractions of complex periodic and chaotic pH-time series in a CSTR mode at different flow rates. Calculations were carried out using the modified mechanism and rate constant values shown in Table 4. Input concentrations were $[\text{H}_2\text{O}_2]_0 = 0.0097$, $[\text{S}_2\text{O}_3^{2-}]_0 = 0.0048$, $[\text{SO}_3^{2-}]_0 = 0.0025$ M, $[\text{H}^+]_0 = 0.0010$ M; $k_0 = 5.00 \times 10^{-4}$ (bottom, P2 oscillations), 5.60×10^{-4} (middle, P4 oscillations), and $6.10 \times 10^{-4} \text{ s}^{-1}$ (top, chaos).

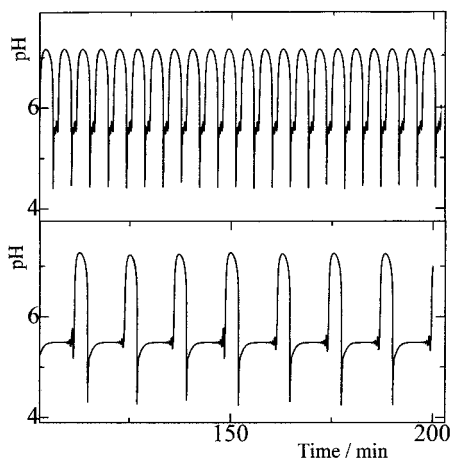


Figure 8. Bursts and P3 pH oscillations in a CSTR calculated by the modified mechanism shown in Table 4. Initial conditions are the same as in Figure 7, but $k_0 = 7.5 \times 10^{-4}$ (bottom, burst) and $k_0 = 6.4 \times 10^{-4} \text{ s}^{-1}$ (top, P3).

Conclusion

Our aim was to design a new chaotic pH oscillator on the basis of the H_2O_2 oxidation of $\text{S}_2\text{O}_3^{2-}$ in a CSTR and to understand its mechanism. Our starting point was an empirical rate law model of the catalyzed reaction proposed by Kurin-Csorgei et al.⁵ We examined the dynamical structure of the model in detail and disclosed that the mechanistic conditions of oscillations and deterministic chaos are inherent in this scheme. According to Beck,⁶ the mechanistic structure of many chemical reactions would support oscillations if the parametric conditions (values of rate constants) were fulfilled. However, the parametric conditions are rarely accomplished in the real chemistry. The lack of the necessary parametric conditions rather

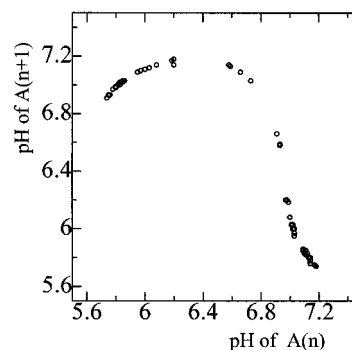


Figure 9. Calculated pH maxima as a function of the pH in the previous maximum (next return map). Calculations were carried out with the model shown in Table 4 using input concentrations and flow rate as in Figure 7 for the chaotic time series (top).

than the lack of the mechanistic conditions makes the oscillatory reactions exotic. We had to face this problem here because the rate constants of the composite reactions are not supportive for periodic behavior in the catalyst-free $\text{H}_2\text{O}_2\text{-S}_2\text{O}_3^{2-}$ reaction and no oscillations can be observed under the studied initial conditions. However, introducing some SO_3^{2-} into the reactor, the contribution of a key reaction (M6) can be increased so that oscillations and chaos can be observed in the experiments. We have performed experiments and simulation calculations in order to disclose the details of this behavior.

We propose a modified mechanism which shows that the complex dynamical behavior is regulated by the changing concentration of H^+ . This reaction is considered as a new member of the family of the pH-regulated chaotic systems.¹² Its chemical mechanism is more complex and less understood than that of the $\text{HCO}_3^-/\text{CO}_3^{2-}$ based chaotic systems.^{13,14} However, neither complex periodic nor chaotic oscillations but only simple periodic behavior can exist in the latter systems unless CO_2 is removed from the reactor through not only the common liquid outflow but also through a separate channel (escape to the air). Such a “perturbation” of the homogeneous chemical reactions by a physical process is not needed for the chaos to appear in the $\text{H}_2\text{O}_2\text{-S}_2\text{O}_3^{2-}\text{-SO}_3^{2-}$ flow system. An obvious special advantage of the present reaction is that chaos is resulted from a pure chemical mechanism.

Acknowledgment. This paper is dedicated to professor Mihály T. Beck on the occasion of his 70th birthday. Gy. R. credits professor Beck for inspiring his interest in the field of oscillating reactions. Financial support was obtained from the Hungarian Science Foundation (OTKA 25076) and from the Japan Society for Promotion of Science.

References and Notes

- (1) Orbán, M.; Epstein, I. R. *J. Am. Chem. Soc.* **1987**, *109*, 101.
- (2) Rábai, Gy.; Epstein, I. R. *J. Am. Chem. Soc.* **1992**, *114*, 1529.
- (3) Strizhak, P. E.; Pojman, J. A. *Chaos* **1996**, *6*, 461.
- (4) Chang, M.; Schmitz, R. A. *Chem. Eng. Sci.* **1975**, *30*, 21.
- (5) Kurin-Csorgei, K.; Orbán, M.; Rábai, Gy.; Epstein, I. R. *J. Chem. Soc., Faraday Trans.* **1996**, *92*, 2851.
- (6) Beck, M. T. A. *C. H. Models in Chemistry* **1992**, *129*, 519.
- (7) Frerichs, G. A.; Thompson, R. C. *J. Phys. Chem. A.* **1998**, *102*, 8142.
- (8) Kaps, P.; Rentrop, P. *Numer. Math.* **1979**, *33*, 55.
- (9) Stanbury, D. M. *Adv. Inorg. Chem.* **1989**, *33*, 69.
- (10) Orbán, M.; Epstein, I. R. *J. Am. Chem. Soc.* **1989**, *111*, 2891.
- (11) Schiller, J. E. *Inorg. Chem.* **1987**, *26*, 948.
- (12) Rábai, Gy. A. *C. H. Models in Chemistry* **1998**, *135*, 381.
- (13) Rábai, Gy.; Hanazaki, I. *J. Phys. Chem. A.* **1996**, *100*, 15454.
- (14) Rábai, Gy.; *J. Phys. Chem. A.* **1997**, *101*, 7085.